Article

Common Semiopen Conformations of Mg-Free Ras, Rho, Rab, Arf, and Ran Proteins Combined with GDP and Their Similarity with GEF-Bound Forms

Kenichi Mori, Masayuki Hata, Saburo Neya, and Tyuji Hoshino

J. Am. Chem. Soc., **2005**, 127 (43), 15127-15137• DOI: 10.1021/ja0467972 • Publication Date (Web): 05 October 2005

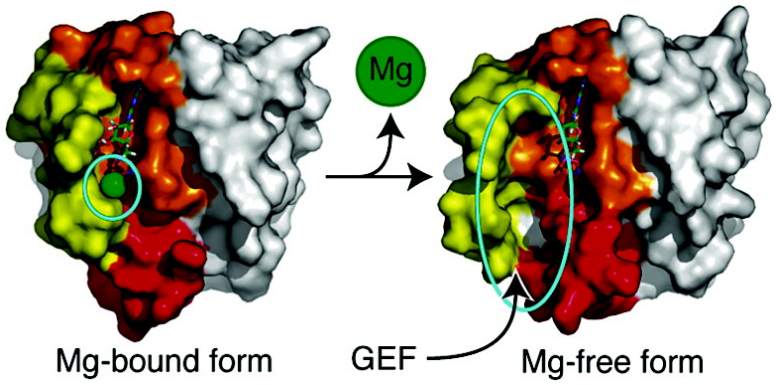

More About This Article

Additional resources and features associated with this article are available within the HTML version:

- Supporting Information
- Links to the 3 articles that cite this article, as of the time of this article download
- Access to high resolution figures
- Links to articles and content related to this article
- Copyright permission to reproduce figures and/or text from this article

View the Full Text HTML

J|A|C|S
ARTICLES
Published on Web 10/05/2005

Common Semiopen Conformations of Mg^{2+}-Free Ras, Rho, Rab, Arf, and Ran Proteins Combined with GDP and Their Similarity with GEF-Bound Forms

Kenichi Mori,*,† Masayuki Hata,† Saburo Neya,† and Tyuji Hoshino†,‡

Contribution from the Department of Physical Chemistry, Graduate School of Pharmaceutical Sciences, Chiba University, 1-33 Yayoi-cho, Inage-ku, Chiba-shi, Chiba 263-8522 Japan, and PRESTO, Japan Science and Technology Agency, 4-1-8 Honcho, Kawaguchi, Saitama, Japan

Received May 31, 2004; E-mail: moriken@graduate.chiba-u.jp

Abstract: A computational study was performed on the Mg^{2+}-free conformations of the small guanine nucleotide-binding proteins (GNBPs): Ras, Rho, Rab, Arf, and Ran, which were complexed with GDP. Molecular dynamics (MD) simulation was executed for each complex for the duration of 3.0 ns to investigate the effects of Mg^{2+} ions on the GNBPs' structure. The results indicated that all Mg^{2+}-free GNBPs formed a groove between the switch region and the nucleotide-binding site. In some GNBP families, the release of Mg^{2+} was reported to play an important role in binding the guanine nucleotide-exchanging factor (GEF) promoting the GDP/GTP exchange reaction. Interestingly, the grooves, which appeared in the MD simulations, were similar to the grooves experimentally observed in the GNBP−GEF complex. We also calculated the Mg^{2+}-bound GNBPs to compare with the Mg^{2+}-free forms. No groove was observed in the Mg^{2+}-bound GNBPs. These results demonstrated a regulatory role of Mg^{2+} ion to prepare a template for the GEF binding. Moreover, the results suggested that the release of Mg^{2+} ion lead to the GEF-GNBP binding.

1. Introduction

Small guanine nucleotide-binding proteins (hereafter referred to as GNBPs) are molecular switches or timers that control a variety of cellular processes.[1,2] Small GNBPs constitute the Ras superfamily that is comprised of five subfamilies: Ras, Rho, Rab, Arf, and Ran.[1] The homology in amino acid sequences among the families is about 30%, and all members of the five subfamilies have a common core structure, which contains five α-helices and six β-sheets (Figure 1). Distinct from the three small GNBP subfamilies, the Arf and the Ran subfamilies have an additional seventh β-sheet. Moreover, the four motifs are conserved in all small GNBPs; the phosphate-binding loop (P-loop) (GXXXXGKS/T), the switch 1 region (YXPT), the switch 2 region (DTAG), and the guanine-binding loop (NKXD and SAK).

Despite their similarities, both in the structure and the sequence, the functions of the small GNBPs extend very widely. Each member of the small GNBPs has been extensively studied through the genetic, cell biological and biochemical approaches, which revealed various functions of the small GNBPs: the Ras family regulates cell proliferation and differentiation,[3,4] morphology,[5] and apoptosis;[6] the Rho family regulates cytoskeletal rearrangement involved in morphology, movement, and behavior;[7−9] the Rab and Arf families regulate intracellular vesicle trafficking;[10] and the Ran family regulates nucleocytoplasmic transport.[11]

The GNBP shifts between the inactive GDP-bound and the active GTP-bound states, where the two proteins, guanine nucleotide exchange factors (GEFs) and GTPase activating proteins (GAPs), promote the switching of the GNBP. Along with these proteins, the guanine nucleotide exchange inhibitors (GDIs) are also involved in the switching cycle,[1] where they inhibit the GDP-GTP exchange and keep the GNBP inactive. GEFs accelerate the exchange of GDP for GTP, that is, the dissociation of GDP from a GNBP and the association of GTP to a GNBP. When a GNBP is in the active state, the GNBP interacts with the proteins in the downstream of the signal transduction. GAPs promote GTP hydrolysis.

Many studies have been carried out to reveal the mechanism of the GEF-mediated exchange reaction. Some kinetic studies demonstrated that GEF-mediated exchange reactions involved GNBP−GEF−nucleotide ternary intermediate formation;[12,13] thus the following mechanism was proposed in Scheme 1.

The ternary complex has a low affinity for a nucleotide; moreover, it initiates a fast conformational change, inducing

† Chiba University.
‡ PRESTO, Japan Science and Technology Agency.

(1) Takai, Y.; Sasaki, T.; Matozaki, T. *Physiol. Rev.* **2001**, *54*, 153.
(2) Vetter, I. R.; Wittinghofer, A. *Science* **2001**, *294*, 1299.
(3) Bar-Sagi, D.; Feramisco, J. R. *Cell* **1985**, *42*, 841.
(4) Hagag, N.; Halegoua, S.; Viola, M. *Nature* **1986**, *319*, 680.
(5) Feramisco, J. R.; Gross, M.; Kamata, M.; Rosenberg, R. W.; Sweet, T. *Cell* **1984**, *38*, 109.
(6) Kauffmann-Zeh, A.; Rodriguez-Viciana, P.; Ulrich, E.; Gilbert, C.; Coffer, P.; Downward, J.; Evan, G. *Nature* **1997**, *385*, 544.
(7) Etienne-Manneville, S.; Hall, A. *Nature* **2002**, *420*, 629.
(8) Yuan, X. B.; Jin, M.; Xu, X.; Song, Y. Q.; Wu, C. P.; Poo, M. M.; Duan, S. *Nat. Cell Biol.* **2003**, *5*, 1.
(9) Etienne-Manneville, S.; Hall, A. *Nature* **2002**, *420*, 629.
(10) Novick, P.; Zerial, M. *Curr. Opin. Cell. Biol.* **1997**, *9*, 496.
(11) Dasso, M. *Curr. Biol.* **2002**, *12*, R502.

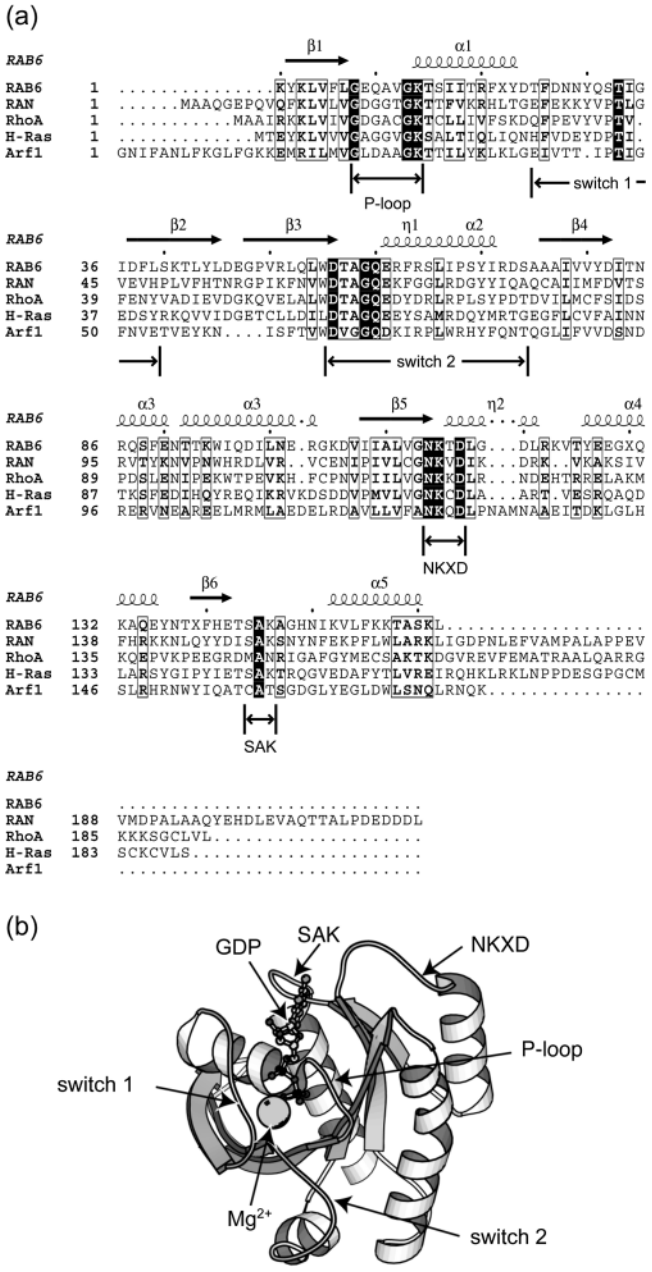

Figure 1. Sequences and core structure of small G-proteins used in our simulations. (a) Full length sequences of Rab6, Ran, RhoA, H-Ras, and Arf1. Consensus sequences: P-loop, the switch 1, the switch 2, and the guanine-binding loops (NKXD and SAK) were labeled. (b) Core structure common to small G-proteins (H-Ras structure depicted as a representative). A Mg^{2+} ion is shown as a sphere. A GDP is shown by a ball-and-stick representation.

the dissociation of the nucleotide. This leads to the formation of a nucleotide-free binary complex. Several crystallographic structures of the nucleotide-free binary GNBP−GEF complexes were reported, where GEFs were found to place their helices or loops to the Mg^{2+}-binding site. The Mg^{2+}-binding site was located in the midst of switch 1, the switch 2, and P-loop, which suggested the disturbance of the Mg^{2+} coordination found in the GDP-bound state had a crucial effect on the GEF-mediated GDP/GTP exchange reaction.[14−17]

Mg^{2+} ion is an essential cofactor for the small GNBPs. In the GDP- and the GTP-bound forms, the Mg^{2+} ion bonds with the protein in an octahedral coordination. The binding affinity of Mg^{2+} ion for GNBPs is low when the Mg^{2+} ion concentration decreases in the micromolar level.[18] It is also known that excess Mg^{2+} ions inhibit the GDP dissociation from GNBPs and, therefore, prevent the binding of GTP with GNBPs.[18−22] The removal of Mg^{2+} ions due to chelating agents increases the GEF activity and their affinity.[12,19] Since the equilibrium constant for the binding of Mg^{2+} ion to GNBP can be measured in experiments,[18] it is natural to consider that not only Mg^{2+}-bound GNBPs are observed but also Mg^{2+}-free ones are found in the solution. The above experimental data suggest that some physiological action would occur in the Mg^{2+}-free GNBPs. However, little is known about the state of Mg^{2+}-free GNBPs. Recently, the crystallographic structure of the Mg^{2+}-free RhoA with GDP was reported,[23] where the switch 1 region was dislocated and became distant from the nucleotide-binding site. The study revealed that the Mg^{2+} ion could regulate the conformation of RhoA, which suggested that Mg^{2+}-free RhoA could be an intermediate of the GEF-mediated GDP/GTP exchange reaction. In addition, it was reported that the release of Mg^{2+} ion preceded the GDP dissociation in the GDP/GTP exchange reaction in Rac, a member of the Rho family.[24] Thus, it is suggested that the Mg^{2+} ion is released before the GDP/GTP exchange reaction in the Rho family. These studies allowed us to speculate that Mg^{2+} ions might regulate conformations of other small G-protein families, yet details of the GNBPs' conformation in the absence of Mg^{2+} ion remain unclear. This was due to the lack of suitable methods to further study the nature of Mg^{2+}-free GNBPs.

To investigate the features of the Mg^{2+}-free GNBPs' conformations, the Mg^{2+}-bound and the Mg^{2+}-free conformations of the GDP-bound GNBPs were calculated using the molecular dynamics (MD) simulations. As a result, the Mg^{2+}-free conformations were found similar to GNBPs in the GEF-binding state. The critical roles of the Mg^{2+} ion in determining the conformations of GNBPs and in binding of GEFs to GNBPs are discussed. In this report, we propose that the GDP dissociation occurs by a stepwise mechanism, where the emergence of the Mg^{2+}-free semiopen GDP form leads to the formation of the GEF−GNBP binary complex.

2. Methods

2.1. Construction of the Initial Structures. The MD simulations were performed on the Mg^{2+}-bound and the Mg^{2+}-free H-Ras, RhoA, Rab6, Arf1, and Ran proteins. The structures of the Mg^{2+}-bound small

(12) Lenzen, C.; Cool, R. H.; Prinz, H.; Kuhlmann, J.; Wittinghofer, A. *Biochemistry* **1998**, *37*, 7420.
(13) Klebe, C.; Prinz, H.; Wittinghofer, A.; Goody, R. S. *Biochemistry* **1995**, *34*, 12543.
(14) Boriack-Sjodin, P. A.; Margarit, S. M.; Bar-Sagi, D.; Kuriyan, J. *Nature* **1998**, *394*, 337.
(15) Goldberg, J. *Cell* **1998**, *95*, 237.
(16) Renault, L.; Kuhlmann, J.; Henkel, A.; Wittinghofer, A. *Cell* **2001**, *105*, 245.
(17) Snyder, J. T.; Worthylake, D. K.; Rossman, K. L.; Betts, L, Pruitt, W. M.; Siderovski, D. P.; Der, C. J.; Sondek, J. *Nat. Struct. Biol.* **2002**, *9*, 468.
(18) John, J.; Rensland, H.; Schlichting, I.; Vetter, I.; Borasio, G. D.; Goody, R. S.; Wittinghofer, A. *J. Biol. Chem.* **1993**, *268*, 923.
(19) Hall, A.; Self, A. J. *J. Biol. Chem.* **1986**, *261*, 10963.
(20) Panniers, R.; Rowlands, A. G.; Henshaw, E. C. *J. Biol. Chem.* **1988**, *263*, 5519.
(21) Pan, J. Y.; Sanford, J. C.; Wessling-Resnick, M. *J. Biol. Chem.* **1996**, *271*, 1322.
(22) Burstein, E. S.; Macara, I. G. *Biochem. J.* **1992**, *282*, 387.
(23) Shimizu, T.; Ihara, K.; Maesaki, R.; Kuroda, S.; Kaibuchi, K.; Hakoshima, T. *J. Biol. Chem.* **2000**, *275*, 18311.
(24) Shutes, A.; Phillips, R. A.; Corrie, J. E.; Webb, M. R. *Biochemistry* **2002**, *41*, 3828.

Scheme 1. GEF-Mediated Exchange Reaction

$$\text{GNBP-GDP} \leftrightarrow \text{GNBP-GDP-GEF} \leftrightarrow \text{GNBP-GEF} \leftrightarrow \text{GNBP-GTP-GEF} \leftrightarrow \text{GNBP-GTP} \quad (1)$$

GNBPs used in our simulation were derived from the X-ray crystallographic structures of the truncated GNBPs in complex with both GDP and Mg^{2+} ion (H-Ras, Protein Data Bank (PDB) code is 4Q21,[25] containing 166 residues; RhoA, 1FTN,[26] containing 177 residues; Rab6, 1D5C,[27] containing 162 residues; chain A of Arf1, 1HUR,[28] containing 180 residues; chain B of Ran, 1BYU,[29] containing 215 residues). The structures of the Mg^{2+}-free GNBPs were constructed by removing the Mg^{2+} ion manually from the respective data. Because the side chain of the arginine residue at the C-terminus of the H-Ras protein was built by the LEaP module of AMBER version 8,[30] the truncated H-Ras has a total of 167 residues. The mutated residue (Asn25) of the RhoA protein was converted to the wild type (Phe25). The selenomethionine residues of the Rab6 protein were also converted to the normal methionines.

Considering the effect of removing the Mg^{2+} ion on the protonation state of the residues in proteins, the pK_a calculation was carried out using MCCE[47] software to examine the pK_a values for all the titratable residues (see the calculated pK_a values in the Supporting Information (Table S1−S5)). The protonation state at pH 7.0 was determined for all the titratable residues, and these residues were renamed to represent the protonation state according to their residue types used in AMBER. This means that GLU, ASP, and HIS were renamed into GLH, ASH, and HIP, respectively, when the pK_a values were greater than 7.0, and HIS and LYS were renamed to HIE or HID and LYN when less than 7.0.

Finally, each complex was solvated with TIP3P water molecules[31] in a cubic box of about 70 Å × 70 Å × 70 Å by the LEaP module. Then, counterions were placed around the proteins so that the net charge was zero in each system, using the LEaP module.

2.2. Details of Computation. The MD simulations were performed with the PMEMD module of AMBER (version 8). All atom ff02[32] force field was used in all MD simulations. A periodic boundary condition was applied, and the pressure was kept constant during the simulation using the Berendsen algorithm.[33] The temperature was kept constant at 300 K. The procedure performed in our simulations was as follows. The system was minimized by the steepest descent method without any constraint for bond length. The additional minimization was executed by the conjugate gradient method. The system was gradually heated from 0 K to 300 K for 56 ps and then kept at 300 K until the atom density of the system was equilibrated. The nonbond interactions were calculated by the Particle Mesh Ewald (PME) method. The cutoff distance for Coulomb and van der Waals forces was 15 Å. To reduce the computational effort, only bond lengths, involving hydrogen atoms, were constrained by the SHAKE method,[34] which allowed the integration time step to be 2 fs. The simulation time was 3.0 ns for each model.

To investigate the influence of the specific protonation states deduced from the pK_a calculation on GNBPs' conformation, the MD simulations were carried out at the default protonation state of AMBER at pH 7.0, where Asp, Glu, Lys, and Arg residues were ionized and His residues were neutral (see calculation results presented in the Supporting Information). The MD simulations described above were repeated for this calculation.

The trajectories were analyzed by the CARNAL and the ptraj modules in AMBER. The mass-weighted B-factors were calculated for each residue by the following equation:

$$B_{res} = \sum_{a=N_{res}}^{N_{res}-1} m_a B_a \Big/ \sum_{a=N_{res}}^{N_{res}-1} m_a$$

$$B_a = \frac{8}{3}\pi^2\langle \delta \mathbf{r}_a^2 \rangle,\ \delta \mathbf{r}_a = \mathbf{r}_a - \langle \mathbf{r}_a \rangle_t \quad (1)$$

where *a* and *res* symbolize the atom number and the residue number, respectively; N_{res} represents the number indicating the first atom in the residue *res*; $\mathbf{r}_a$ and m_a represent the coordinate and the mass of each atom, respectively. The brackets represent the time average.

The B-factors were analyzed using the software R (version 2.0), where the sample cross correlation between the calculated B-factor and the crystallographic temperature factor was calculated by the following equation

$$R = \frac{C(y, z)}{C(y, y)C(z, z)}$$

$$C(y, z) = \frac{1}{T}\sum_{t=1}^{T}(y_t - y_y)(z_t - \mu_z) \quad (2)$$

where *R* and *C* represent a sample cross correlation and a sample cross covariance, respectively; *T* represents the number of residues; *y* and *z* denote the data sets containing B-factors and temperature factors of all the residues; μ_y and μ_z represent the averages of *y* and *z*, respectively. *R* can vary in the range from −1 to 1; hence, the two variables, *y* and *z*, have a strong positive correlation when *R* is close to 1.

All graphical figures were produced using the programs MolScript,[35] MOLMOL,[36] and GRASP.[37] Solvent accessible surface areas were calculated with MOLMOL.

3. Results

3.1. Comparison of MD Simulations of Mg^{2+}-Bound GNBPs with Experimental Data. To check the consistency between the simulations and the experiments, the root-mean-square deviations (RMSD) of the Mg^{2+}-bound GNBPs from each X-ray crystallographic structure were calculated (Table 1 and Figure S1 in the Supporting Information). Table 1 shows that the RMSDs of all GNBPs were approximately 1.2 Å and the standard deviations were small, which indicates that the structures obtained from the simulations were stable and compatible with the corresponding crystallographic structures.

In addition to RMSD, B-factors of each Mg^{2+}-bound GNBP were calculated using the results of the MD simulation and were compared with the temperature factors of each X-ray crystallographic structure in order to examine whether our simulations reproduced the atom fluctuation in the experiment (Table 2 and Figure S2 in the Supporting Information). Table 2 shows the sample cross correlations between the calculated B-factors and the experimental temperature factors. Although the B-factors

(25) Milburn, M. V.; Tong, L. A.; de Vos, A. M.; Brunger, A.; Yamazaki, Z.; Nishimura, S.; Kim, S. H. *Science* **1990**, *247*, 939.
(26) Wei, Y.; Zhang, Y.; Derewenda, U.; Liu, X.; Minor, W.; Nakamoto, R. K.; Somlyo, A. V.; Somlyo, A. P.; Derewenda, Z. S. *Nat. Struct. Biol.* **1997**, *4*, 699.
(27) Chattopadhyay, D.; Langsley, G.; Carson, M.; Recacha, R.; DeLucas, L.; Smith, C. *Acta Crystallogr., Sect. D* **2000**, *56*, 937.
(28) Amor, J. C.; Harrison, D. H.; Kahn, R. A.; Ringe, D. *Nature* **1994**, *372*, 704.
(29) Stewart, M.; Kent, H. M.; McCoy, A. J. *J. Mol. Biol.* **1998**, *284*, 1517.
(30) Case, D. A. et al. *AMBER 8*; University of California, San Francisco, 2004.
(31) Jorgensen, W. L.; Chandrasekhar, J.; Madura, J.; Klein, M. L. *J. Chem. Phys.* **1983**, *79*, 926.
(32) Wang, J.; Cieplak, P.; Kollman, P. A. *J. Comput. Chem.* **2000**, *21*, 1049.
(33) Berendsen, H. J. C.; Postma, J. P. M.; van Gunsteren, W. F.; DiNola, A.; Haak, J. R. *J. Chem. Phys.* **1984**, *81*, 3684.
(34) Ryckaert, J. P.; Ciccotti, G.; Berendsen, H. J. C. *J. Comput. Phys.* **1977**, *23*, 327.
(35) Kraulis, P. J. *J. Appl. Crystallogr.* **1991**, *24*, 946.
(36) Koradi, R.; Billeter, M.; Wuthrich, K. W. *J. Mol. Graph.* **1996**, *14*, 51.
(37) Nicholls, A.; Sharp, K.; Honig, B. *Proteins* **1991**, *11*, 281.

Table 1. Root Mean Square Deviations of the Mg^{2+}-Bound GNBPs from Each Crystallographic Structure[a]

	pK_a-PDB	default-PDB
H-Ras	1.15 ± 0.05	1.26 ± 0.09
RhoA	1.29 ± 0.11	0.90 ± 0.08
Rab6	1.17 ± 0.07	1.35 ± 0.11
Arf1	1.47 ± 0.24	1.33 ± 0.08
Ran	1.20 ± 0.08	1.19 ± 0.06

[a] Unit is Å. 750 sets of coordinates for the last 1.5 ns simulation (acquired every 2 ps) were used for statistics. pK_a-PDB represents the sample cross correlation values between the B-factors in the pK_a-determined protonation state and the experimental temperature factors. The default-PDB represents the values between the B-factors in the default protonation state of AMBER and the experimental ones.

Table 2. Sample Cross Correlation Values between the Calculated B-Factors and the Experimental Temperature Factors of Mg^{2+}-Bound GNBPs[a]

	pK_a-PDB	default-PDB
H-Ras	0.61	0.68
RhoA	0.60	0.67
Rab6	0.60	0.53
Arf1	0.48	0.58
Ran	0.70	0.78

[a] The last 1.5 ns simulation (acquired every 2 ps), 750 sets of coordinates, was used for statistics.

and the temperature factors do not match perfectly due to the difference in the experimental and the computational conditions, the data suggested that the computational results had positive correlations with the experimental temperature factors (Table 2).

These results demonstrate the success of the simulations in reproducing the characteristics of the GNBPs' structural properties.

3.2. B-Factors of H-Ras, RhoA, Rab6, Arf1, and Ran. To investigate the residues where large conformational changes occurred, we examined the average B-factor using the pK_a-determined protonation state (Figure 2). The B-factors of Mg^{2+}-free H-Ras were largely different from those of Mg^{2+}-bound H-Ras, prominently in the switch 1 region (the residue number of 25−40) (Figure 2a). In particular, Asp33 had the largest B-factor value in the Mg^{2+}-free form, which was approximately five times larger than that in the Mg^{2+}-bound form. Tyr32 to Tyr40 also largely fluctuated in the Mg^{2+}-free form. In the Mg^{2+}-bound form, the switch 2 region had the largest B-factor, which was consistent with the crystallographic data.[25] This result also demonstrated the success of performing the simulation correctly and adequately having similar results to the experiments. The B-factors of RhoA in the Mg^{2+}-free form were larger than those of the Mg^{2+}-bound form at the region from switch 1 to the N-terminal side of switch 2 (the residue number of 27−63) (Figure 2b). As for Rab6, the switch 1 region (the residue number of 33-48) had large B-factor values in the Mg^{2+}-free form. These results indicated that the absence of Mg^{2+} ions caused large fluctuations around the switch 1 regions of H-Ras, RhoA, and Rab6. The B-factors of Arf1 and Ran were different, compared with the other three GNBPs (Figure 2d and 2e). Both Mg^{2+}-free GNBPs had larger fluctuations in the regions between the switch 1 and switch 2 regions (the residue number of 55−61 in Arf1, 49−58 in Ran). In addition, there were high peaks of B-factors around the C-terminal region of switch 2 (the residue number of 55−61) and the residue number of 130−

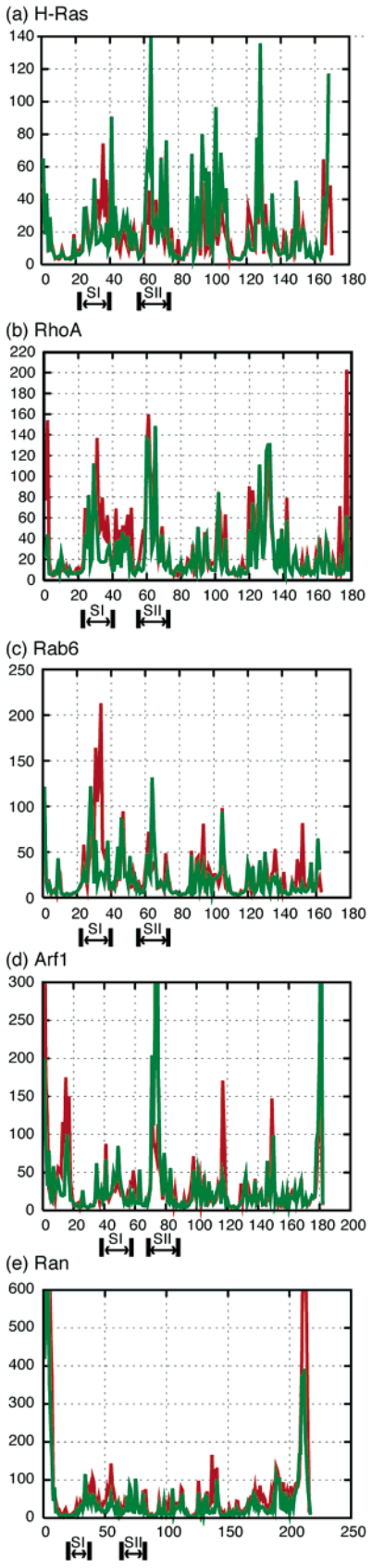

Figure 2. B-factors of Mg^{2+}-bound and Mg^{2+}-free H−Ras, RhoA, Rab6, Arf1, and Ran, in unit of $Å^2$. The abscissa represents the residue number. The green line represents the Mg^{2+}-bound form and the red line represents the Mg^{2+}-free form. SI and SII denote the switch 1 and 2 regions. 750 sets of coordinates for the last 1.5 *ns* simulation (acquired every 2 *ps*) were used for calculation.

Table 3. Average Distances between the GDP-Pβ Atom and the Cα Atoms on the Switch 1 Region[a]

		Y[a]	X[a]	P[a]	T[a]
H-Ras	Mg(+)[b]	6.22 ± 0.26	6.74 ± 0.28	7.35 ± 0.63	10.52 ± 0.48
	Mg(−)[b]	6.79 ± 0.48	8.69 ± 0.41	10.94 ± 0.49	13.64 ± 0.43
RhoA	Mg(+)	10.72 ± 0.39	8.24 ± 0.56	6.62 ± 0.41	6.59 ± 0.22
	Mg(−)	12.38 ± 0.45	12.41 ± 0.85	11.22 ± 0.79	12.79 ± 0.95
Rab6	Mg(+)	10.60 ± 0.43	7.37 ± 0.30	8.05 ± 0.41	5.45 ± 0.35
	Mg(−)	11.15 ± 0.53	12.73 ± 0.66	11.10 ± 1.05	9.72 ± 1.16
Arf1	Mg(+)	14.41 ± 0.40	18.87 ± 0.45	20.67 ± 0.42	18.52 ± 0.60
	Mg(−)	14.43 ± 0.40	19.08 ± 0.42	21.34 ± 0.44	18.82 ± 0.49
Ran	Mg(+)	18.54 ± 0.27	16.84 ± 0.27	18.51 ± 0.60	19.59 ± 0.44
	Mg(−)	19.60 ± 0.43	18.20 ± 0.52	20.09 ± 0.79	21.10 ± 0.54

[a] The unit is Å. 500 sets of coordinates for the last 1 ns simulation (acquired every 2 ps) were used for statistics. [a] YXPT stands for Tyr32, Asp33, Pro34, and Thr35 in H-Ras; Tyr30, Val35, Pro36, and Thr37 in RhoA; Tyr40, Gln41, Ser42, and Thr43 in Rab6; Thr45, Ile46, Pro47, and Thr48 in Arf1; Tyr39, Val40, Pro41, and Thr42 in Ran, respectively. [b] Mg(+) and Mg(−) mean whether a Mg^{2+} ion is present or not.

140. At the C-terminal region (the residue number of 187−215) in Mg^{2+}-free Ran, a high peak was also detected.

Figure S3 in the Supporting Information shows the B-factors calculated with the AMBER default ionization state. It should be noted that the profiles of the B-factors of H-Ras and Rab6 were similar to those calculated with the pK_a-determined protonation state where the B-factors at the switch 1 regions were large. As for RhoA, no prominent difference was seen between the Mg^{2+}-bound and the Mg^{2+}-free forms. Mg^{2+}-free Arf1 had large B-factor values at switch 1 and the switch 2 regions, as compared to the Mg^{2+}-bound form. In Mg^{2+}-free Ran, there were high peaks of B-factors at the region of the residue number of 130−140 and at the C-terminal region, which resembled the result of Ran in the case of using a pK_a-determined protonation state. These results demonstrate that the switch regions are very sensitive to the Mg^{2+} ion removal.

3.3. Conformations of Switch 1. Table 3 and Figure 3 show the computational results on switch 1 conformations of the Mg^{2+}-bound and -free GNBPs. The switch 1 region of the Mg^{2+}-free H-Ras traveled outside to detach from the GDP binding site, compared to the Mg^{2+}-bound form. In particular, Pro34 and Thr35, the last two residues of the YXPT motif, largely shifted outward with no less than 3−4 Å and did not participate in the nucleotide recognition. Moreover, the first two residues, Tyr32 and Asp33, were translocated from the original site. Phe28, which recognizes the guanine base of the GDP, did not change its location. When the AMBER default protonation state was incorporated, the conformational change of switch 1 was exaggerated (Figure S4a in the Supporting Information). The deviations of Pro34 and Thr35 were 6−11 Å, accompanied by a large translocation of Tyr32 and Asp33. These results suggested that the lack of Mg^{2+} ion from H-Ras induced the conformational rebuilding of the switch 1 region, especially at the YXPT motif.

In the case of RhoA, the structure of the switch 1 region of the Mg^{2+}-free form was prominently distinct from that of the Mg^{2+}-bound form (Figure 3b). In the Mg^{2+}-free form, Thr37 (Thr35 in H-Ras), which is a member of the ligands coordinated to the Mg^{2+} ion in RhoA, moved approximately 6 Å from the Mg^{2+}-binding site (Table 3). After Thr37 shifted, Pro36 began to move and became distant from the Mg^{2+}-binding site by 4.5 Å. The distances from the other two residues to GDP in Mg^{2+}-free RhoA were larger than the Mg^{2+}-bound form. Therefore, the switch 1 region became more distant from GDP in the Mg^{2+}-free form, while the region kept close to the GDP binding site in the Mg^{2+}-bound form. A similar result was obtained when the AMBER default protonation state was used (Figure S4b). These results indicated that the removal of Mg^{2+} ion had a remarkable influence on the conformation of switch 1 in RhoA.

The switch 1 region of Rab6 had the largest amount of conformational changes among all of GNBPs (Table 3 and Figure 3c). In the Mg^{2+}-free form, the distance between Thr43 (Thr35 in H-Ras) and the Mg^{2+}-binding site resulted in 9.7 Å, while the Mg^{2+}-bound form kept its distance with Thr35 at 5.5 Å during the simulation. Moreover, Tyr40, Gln41, and Ser42 (Tyr32, Asp33, and Pro34 in H-Ras) moved 1.2 Å, 5.5 Å, and 3 Å away from the nucleotide-binding site in the absence of Mg^{2+} ion. Like H-Ras, an exaggerated result was obtained when using the AMBER default protonation state (Figure S4c). These results revealed that the Mg^{2+} ion played a key role to keep switch 1 closed in Rab6, similar to H-Ras.

When Mg^{2+}-bound and -free Arf1 were calculated with the pK_a-determined protonation state, they did not exhibit any obvious conformational change in the switch 1 region (Table 3 and Figure 3d). Nevertheless, when in the AMBER default state, the most prominent conformational change among all GNBPs was observed in Mg^{2+}-free Arf1 (Figure S4d). Phe51, which was reported as a critical residue for the interaction with Gea2 (a GEF of Arf1),[15] was disclosed from the interior of the protein and was exposed to solvent in the Mg^{2+}-free form. In addition, the β-sheet comprising the switch 1 region of Arf1 was shortened by the absence of Mg^{2+} ion and changed its conformation to a loop shape. This result was consistent with the report indicating that the switch 1 region in the Arf1−Gea2 complex was completely a loop structure.[15] The large conformational difference was derived from a hinge motion at Thr43 and Thr44 (Tyr32 in H−Ras), which was located at the N-terminus of the YXPT motif (TIPT in Arf1; the residue number: 44-47) of switch 1. The torsion angles of Thr43 and Thr44 (φ, ψ) = (−139.9°, 135.1°) in the Mg^{2+}-bound form changed to (φ, ψ) = (−69.7°, 153.6°) in the Mg^{2+}-free form.

As for Ran, the secondary structure of the GDP−Mg^{2+}-bound form in the crystal structure was quite similar to Arf1, where they had seven β-strands and switch 1 consists of two β-strands. Interestingly, our computational results revealed that the conformational change of the switch 1 region was compatible between Ran and Arf1; that is, Mg^{2+}-free Ran barely deviated from the Mg^{2+}-bound form (Figures 3e and S4e). There was only a small displacement in switch 1, where it slightly moved away from the Mg^{2+}-binding site due to the conversion from the Mg^{2+}-bound to the Mg^{2+}-free form.

3.4. Conformations of Switch 2. The switch 2 regions in Mg^{2+}-bound and -free H-Ras had a prominent difference at the DTAG motif and its adjacent region containing a loop and an α-helix (Figure 4a). Ala59 approached the Mg^{2+}-binding site (Table 4), which was consistent with the X-ray crystallographic structure of the H-Ras−SOS complex.[14] Asp57 and Thr58, which formed hydrogen bonds with water molecules and stabilized the coordination of Mg^{2+} ion via these water molecules in the Mg^{2+}-bound form, were detached from GDP (Table 4) and altered their torsion angles ($\Delta\psi$ was 50° and −30°, respectively) in the Mg^{2+}-free form. It was also found that

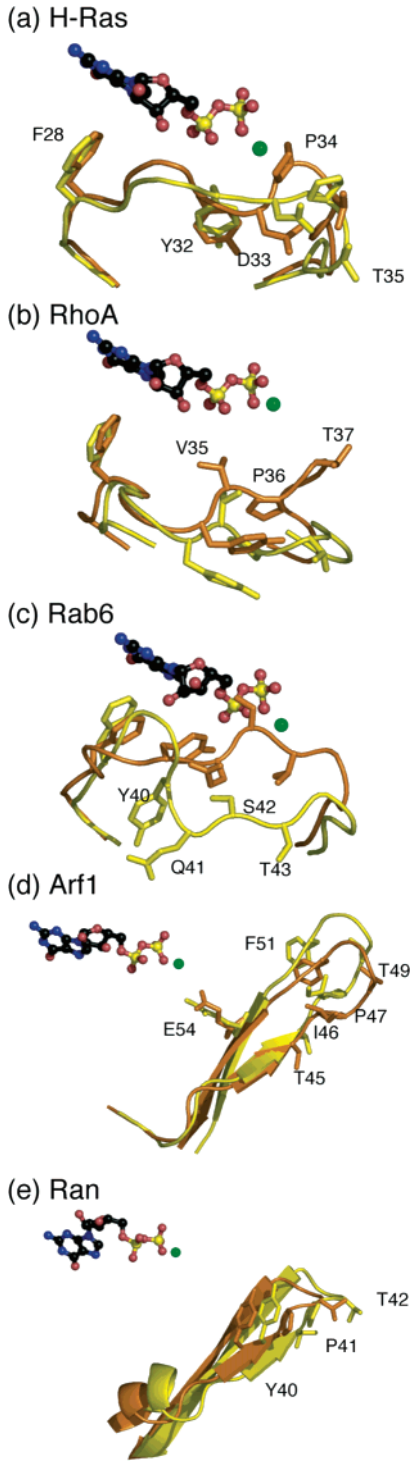

Figure 3. Comparison of the conformations of the switch 1 region between Mg^{2+}-free and Mg^{2+}-bound forms. The Mg^{2+}-free and -bound forms are drawn in yellow and orange, respectively. (a) H-Ras (residues 25−40), (b) RhoA (residues 27−42), (c) Rab6 (residues 33−48), (d) Arf1 (residues 39−56), (e) Ran (residues 32−47).

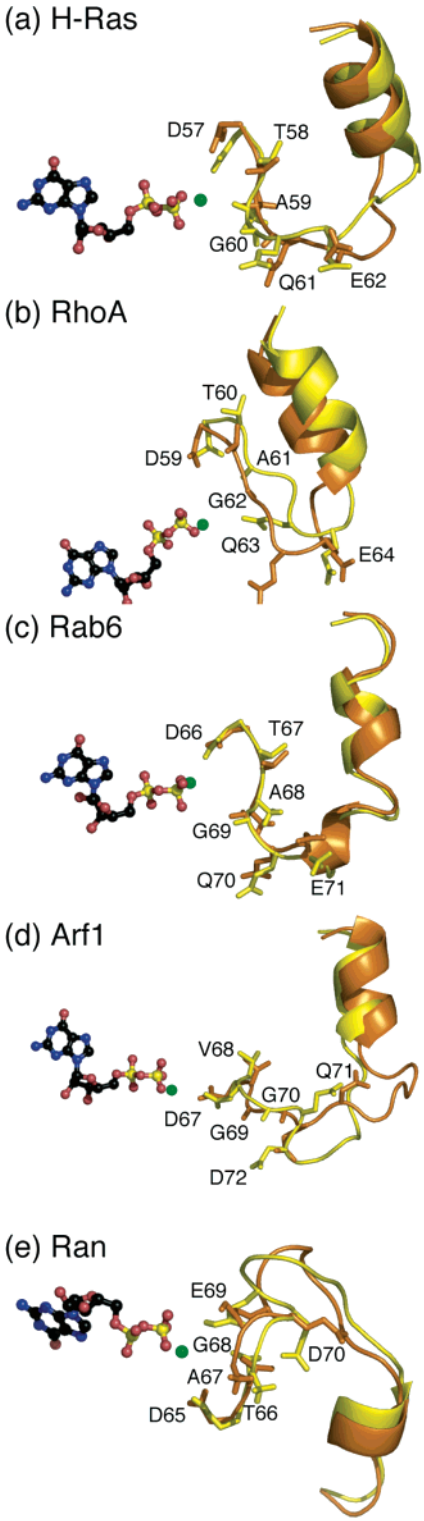

Figure 4. Comparison of the conformations of the switch 2 region between Mg^{2+}-free and Mg^{2+}-bound forms. Coloring method is the same as that in Figure 3. (a) H-Ras (residues 57−75), (b) RhoA (residues 59−77), (c) Rab6 (residues 66−84), (d) Arf1 (residues 67−85), (e) Ran (residues 65−83).

these changes of Asp57 and Thr58 preceded the movement of Ala59. Hence, these two residues, which were located at the hinge of the switch 2 region in H-Ras, induced the movement of Ala59.

Switch 2 in RhoA had the largest conformational change among all of GNBPs (Figure 4b). All of the four residues in the DTAG motif shifted away from GDP (Table 4). Asp59 and Thr60 (Asp57 and Thr58 in H-Ras) exhibited large torsion changes similar to H-Ras, while Ala61 (Ala59 in H-Ras) detached from the Mg^{2+}-binding site in contrast to H-Ras.

In the case of Rab6 in the Mg^{2+}-free form, the switch 2 region resulted in some conformational changes, but scarcely moved from the initial position (Figure 4c). Asp66 (Asp57 in H-Ras)

Table 4. Average Distances between the GDP-Pβ Atom and the Backbone Oxygen Atoms on the Switch 2 Region

		D[a]	T[a]	A[a]	G[a]
H-Ras	Mg(+)[b]	7.94 ± 0.27	5.67 ± 0.19	8.19 ± 0.42	10.31 ± 0.36
	Mg(−)[b]	9.75 ± 0.26	7.19 ± 0.36	6.89 ± 0.80	10.80 ± 0.37
RhoA	Mg(+)	9.88 ± 0.23	5.71 ± 0.20	8.88 ± 0.31	10.13 ± 0.50
	Mg(−)	10.68 ± 1.04	9.22 ± 0.80	11.36 ± 0.77	12.52 ± 1.04
Rab6	Mg(+)	10.63 ± 0.22	6.02 ± 0.19	5.87 ± 0.41	8.14 ± 0.26
	Mg(−)	9.03 ± 0.30	6.18 ± 0.43	8.13 ± 0.52	8.26 ± 0.36
Arf1	Mg(+)	9.65 ± 0.21	9.57 ± 0.29	14.08 ± 0.46	16.45 ± 0.72
	Mg(−)	9.73 ± 0.21	10.43 ± 0.23	14.22 ± 0.33	17.55 ± 0.40
Ran	Mg(+)	9.51 ± 0.25	7.04 ± 0.22	8.91 ± 0.73	9.04 ± 0.60
	Mg(−)	10.78 ± 0.41	8.02 ± 0.42	10.40 ± 0.64	10.38 ± 0.44

[a] DTAG means Asp57, Thr58, Ala59, and Gly60 in H-Ras; Asp59, Thr60, Ala61, and Gly62 in RhoA; Asp66, Thr67, Ala68, and Gly69 in Rab6; Asp67, Val68, Gly69, and Gly70 in Arf1; Asp65, Thr66, Ala67, and Gly68 in Ran, respectively. [b] Mg(+) and Mg(−) represent whether a Mg^{2+} ion is present or not. [c] The unit is Å. 500 sets of coordinates for the last 1 ns simulation (acquired every 2 ps) were used for statistics.

approached toward GDP by 1.6 Å (Table 4), and Ala68 (Ala59 in H−Ras) moved away from GDP by 2.3 Å. As a result, switch 2 was kept at the original position.

As for Mg^{2+}-free Arf1 and Ran, the residues at the DTAG motifs detached slightly from GDP (Figures 4d and 4e). The switch 2 region shifted away from the Mg^{2+}-binding site by approximately 0.6 Å and 1.3 Å in Mg^{2+}-free Arf1 and Ran, respectively. However, these changes were relatively small compared to H-Ras, RhoA, and Rab6.

In all GNBPs, the conformational changes of the switch 2 were exaggerated when the AMBER default protonation state was used (Figure S5), which was similar to the result of the switch 1 region.

3.5. Overall Structural Changes from the Viewpoint of Molecular Surface and Solvent Accessible Surface Areas. GNBPs' molecular surfaces after the simulation were shown in Figure 5. The solvent accessible surface areas (SASA) were calculated (Table S6 in the Supporting Information). Due to the high flexibility of the switch 1 region (Figure 2 a), the whole structure of H-Ras had a groove between the switch 1 and the GDP binding site in the Mg^{2+}-free form (Figure 5a). Furthermore, in the case of using the AMBER default protonation state, a groove was also created around the GDP binding site due to the movement of the switch 1 loop, which doubled the SASA of GDP in the absence of Mg^{2+} ion.

Similarly, the removal of Mg^{2+} ion from RhoA created a groove between the C-terminus of the switch 1 region and the middle of the switch 2 region (Figure 5 b). The SASA was increased by 309 $Å^2$ as a result of the formation of the groove. In contrast, any groove cannot be observed in the case of using the AMBER default protonation state, and consequently the SASA was decreased.

In Rab6, on the other hand, the absence of the Mg^{2+} ion created a groove between the GDP binding site and the switch 1 region (Figure 5c). The conserved motif regions of P-loop, switch 1 and 2, NKXD, and SAK surrounded this groove. A similar groove was observed in the calculation with the AMBER default protonation state. According to the creation of the grooves, the SASAs of Mg^{2+}-free Rab6 increased by 274 $Å^2$ and 419 $Å^2$ in the pK_a-determined and the AMBER default protonation states, respectively.

The appearance of a groove found in Mg^{2+}-free Arf1 was not obvious in the pK_a-determined protonation state while clearly observed in the AMBER default state (Figure 5d). Although there was little difference in the conformation between the Mg^{2+}-bound and the Mg^{2+}-free forms in the pK_a-determined protonation state, the SASA increased by 190 $Å^2$. The changes of the SASA around the switch 1 and the switch 2 regions contributed to this increase of the SASA. In the AMBER default protonation state, it should be noted that the SASA increased by no less than 800 $Å^2$. This increase of the SASA was mainly due to the switch 1 conversion from the β-sheet conformation to the loop shape in the absence of the Mg^{2+} ion. In particular, the exposure of Phe51 to the solvent contributed to the increase of the SASA, because the SASA of Phe51 changed from 45.5 to 157.5 $Å^2$. The motion of Phe51 was fundamentally derived from the structural change in switch 1.

In the case of Ran, no clear groove was seen in the Mg^{2+}-bound and -free forms in the pK_a-determined protonation state, while the creation of a groove was found in the AMBER default state (Figure 5e). Despite the absence of the groove, the SASA increased by 327 $Å^2$, which was similar to the case of Arf1 as described above. In the AMBER default protonation state, Mg^{2+}-free Ran made a groove between the NBD and the switch 2 region, while other GNBPs exhibited the conformational change mainly at the switch 1 regions. As a result, the SASA increased by 241 $Å^2$.

4. Discussion

We calculated Mg^{2+}-bound and Mg^{2+}-free H-Ras, RhoA, Rab6, Arf1, and Ran proteins and compared their conformations to reveal the role of the Mg^{2+} ion on regulating GNBPs' structures. Our results showed that the lack of the Mg^{2+} ion induced large conformational changes in the switch regions. Although the switch regions intrinsically had dynamic properties, our results demonstrated that the lack of Mg^{2+} ion enhanced the mobility of the switch regions as shown in the B-factor values (Figure 2). Due to the increase of the mobility, the large conformational changes occurred around the GDP binding site (Figures 3, 4, S4, and S5). The Mg^{2+}-bound and -free GNBPs were also calculated under the default protonation state of AMBER at pH 7.0, where all Asp and Glu residues were anionic, and Lys and Arg residues were cationic, and His residues were neutral (HID, which is protonated at the δ position), regardless of the presence or the absence of Mg^{2+} ion. Namely, the protonation state between the Mg^{2+}-bound and -free forms was the same. The AMBER default protonation state exaggerated the fluctuation and the conformational changes in the absence of the Mg^{2+} ion (Figure S3, S4, S5). Switch 1 and 2 fluctuated much more than the other regions, which resulted in producing distinct differences between the Mg^{2+}-bound and -free forms. The characteristic grooves were also created in Arf1 and Ran (Figure 5). This demonstrated that the conformational changes were sensitive to the protonation state of the residues.

In four of the five GNBPs (except for Arf1), the removal of Mg^{2+} ion extremely affected the pK_a value of Asp residue at the GDP-binding site (shown in Table S1: Asp57 in H-Ras; Asp59 in RhoA; Asp65 in Rab6; Asp66 in Ran). These Asp residues were close to the phosphate moiety of GDP and were buried in the proteins. This environment would cause the Asp residue to be neutral, because the neutral state of an Asp or a

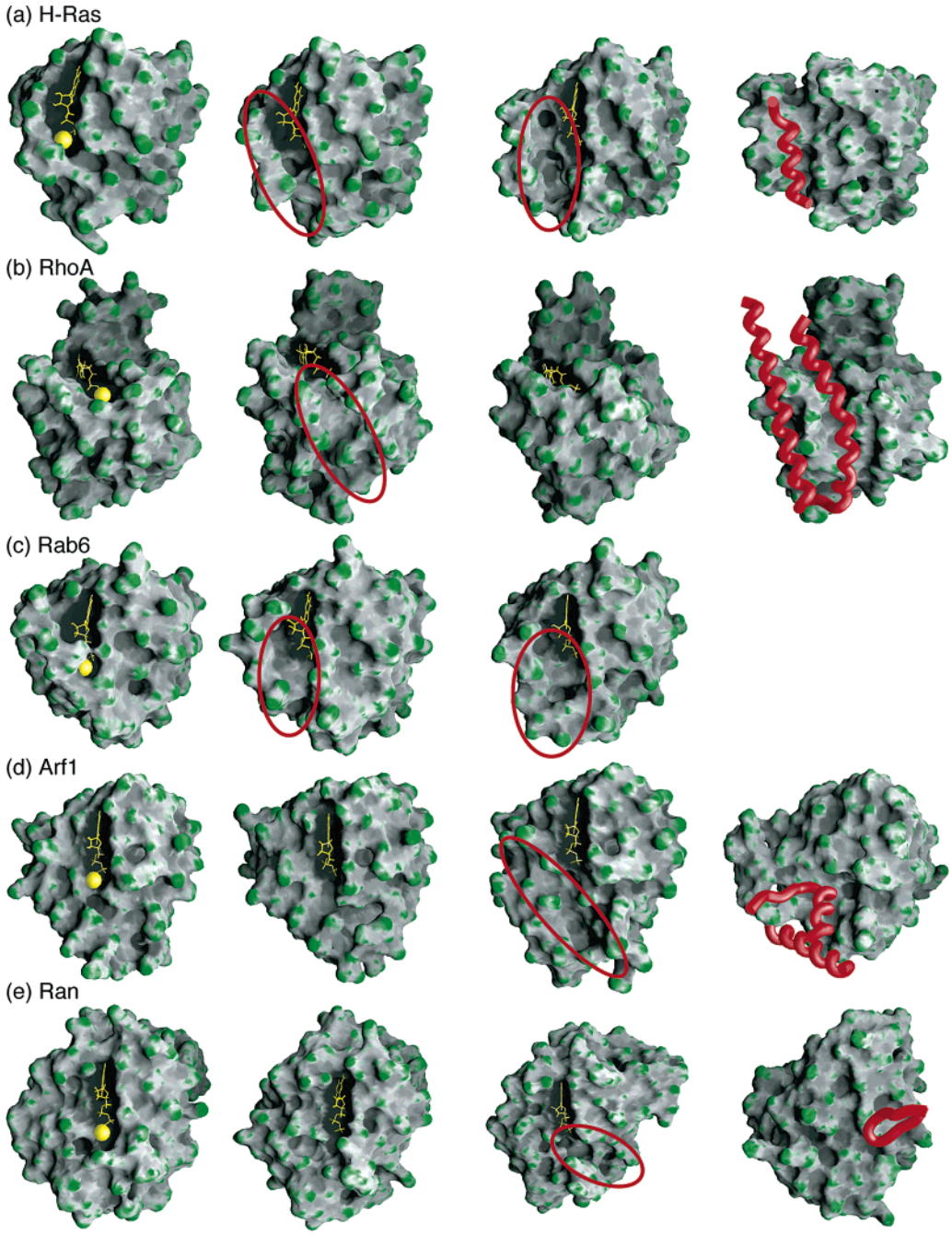

Figure 5. Molecular surfaces for the time-averaged structure of the Mg^{2+}-bound and Mg^{2+}-free GNBPs (Left, the Mg^{2+}-bound form; middle-left, the Mg^{2+}-free form (pK_a-determined protonation state); middle-right, the Mg^{2+}-free form (AMBER default protonation state); right, the GEF-bound form obtained experimentally). The GEF-bound form for Rab6 is unavailable. GDPs and Mg^{2+} ions are represented by the sticks and the spheres colored yellow. The helices or loops of GEFs interacting with GNBPs are represented as red tubes. Red circles indicate the grooves appearing due to the lack of the Mg^{2+} ion. These structures are the final 0.2 ns averages of the MD simulations.

Glu residue is more stable in the hydrophobic environment. In the case of Arf1, Glu54 was noticeably affected, and its pK_a value was larger than 7.0. Although Asp67 located on switch 2 was also affected, it remained to be acidic. Hence the removal of the Mg^{2+} ion would change the protonation state around the GDP-binding site. The protonation state of the Asp or Glu residue near the GDP-binding site will influence the switch conformations.

To investigate the cause for the switch motion, H-Ras was chosen as a representative of the GNBPs, and the quantum chemical calculation was performed using the FMO (fragment molecular orbital) method. The fundamental concept of the FMO method is to divide the protein into the fragments consisting of one or two residues, which enables the quantum chemical calculation of the whole part of the protein.[48] The FMO

(38) Farnsworth, C. L.; Feig, L. A. *Mol. Cell. Biol.* **1991**, *11*, 4822.
(39) De Vendittis, E.; Zahn, R.; Fasano, O. *Eur. J. Biochem.* **1986**, *161*, 473.
(40) Barstein, E. S.; Brondyk, W. H.; Macara, I. G. *J. Biol. Chem.* **1992**, *267*, 22715.
(41) Kornbluth, S.; Dasso, M.; Newport, J. *J. Cell Biol.* **1994**, *125*, 705.
(42) Zhang, B.; Zhang, Y.; Wang, Z.; Zheng, Y. *J. Biol. Chem.* **2000**, *275*, 25299.
(43) Pan, J. Y.; Wessling-Resnick, M. *Bioessays* **1998**, *20*, 516.
(44) Landino, L. M.; Macdonald, T. L. *J. Inorg. Biochem.* **1997**, *66*, 99.
(45) Scheffzek, K.; Stephan, I.; Jensen, O. N.; Illenberger, D.; Gierschik, P. *Nat. Struct. Biol.* **2000**, *7*, 122.
(46) Hall, B. E.; Yang, S. S.; Boriack-Sjodin, P. A.; Kuriyan, J.; Bar-Sagi, D. *J. Biol. Chem.* **2001**, *276*, 27629.

calculation revealed the existence of a large repulsive energy between the switch regions and GDP (Figure S6). This result suggested that the repulsion energy between the switch region and GDP would force the switch region to move away from the GDP-binding site. Because of the positive charge of the Mg^{2+} ion and its interaction with the main chain or the side chain atoms in the switch regions, the Mg^{2+} ion buffered these repulsive interactions in the Mg^{2+}-bound form. Accordingly the removal of the Mg^{2+} ion increased the fluctuation of the switch regions in our MD calculations.

Our computational results can be compared with the experimental structures for the GNBPs complexed with the respective GEFs, where the GNBPs lacked the Mg^{2+} ion and the guanine nucleotide and exhibited large conformational changes in the switch regions. The solvent accessible surfaces of the Mg^{2+}-bound, the Mg^{2+}-free, and the GEF-bound GNBPs are shown in Figure 6. In H-Ras, our calculations indicated that the absence of the Mg^{2+} ion made a groove between the nucleotide-binding domain (NBD) and the switch 1 region (Figure 5a). It should be noted that such a groove was found in the H-Ras bound to the Cdc25 domain of Son of sevenless (SOS) (Ras-GEF),[14] where there was no Mg^{2+} ion; moreover, a conformational change appeared in the switch 1 region (Figure 6a). A striking similarity between the two structures was the switch 1 region located apart from the nucleotide-binding site. This conformation represented the opening of the pocket where SOS inserted an α-helix to make a Ras−SOS complex. The transformation of the pocket into the Ras open form induced by SOS increased the solvent accessible surface areas around the nucleotide-binding site consisting of the conserved motif regions (P-loop, switch 1 and 2, NKXD, and SAK). This had also been observed in our calculation. In addition, when Asp57 of H-Ras was negatively charged, the conformational change was exaggerated (Figure 5a). The superposition of the structure of Mg^{2+}-free H-Ras on the SOS-bound form gave the root-mean-square deviation (RMSD) value of 2.5 Å or 2.0 Å when excluding the switch 2 regions for RMSD estimation. On the other hand, the RMSD excluding the switch 2 region was 3.0 Å between Mg^{2+}-bound and SOS-bound H-Ras. These results indicated that the absence of the Mg^{2+} ion induced the conformation of H-Ras to resemble SOS-bound H-Ras, especially for the conformation of the switch 1 region.

As for Mg^{2+}-free RhoA, a groove that appeared due to the absence of the Mg^{2+} ion was located on the region between the C-terminus of switch 1 and switch 2 whichever the default or the pK_a-determined protonation state was used (Figure 6b). Surprisingly, the binding site of Dbl (Rho−GEF) was also at the same position (Figure 6b), where Dbl interacted with RhoA through the α-helix.[17]

In the case of Ran and Arf1, the switch region moved slightly away from the GDP-binding site (Figure 6d and 6e). When the AMBER default protonation state was used, the appearance of the grooves was clearly observed in these proteins in their Mg^{2+}-free forms. In the case of Ran, similar to H-Ras and RhoA, the position of the groove was identical with the interaction site of Ran−RCC1 (Ran−GEF), where RCC1 inserted a loop in it (Figure 6e). In the absence of the Mg^{2+} ion, Arf1 exhibited the large conformational change in the switch 1 region, which induced the deformation in the seventh β-sheet; moreover, Phe51 was exposed to the solvent from the inside of the protein (Figure 6d). It should be emphasized that the conversion of the switch 1 region into a loop conformation and the exposure of Phe51 were also found in the Arf1−Gea2 complex[15] (Figure 6d). Switch 1 completely formed a loop in the Arf1−Gea2 complex. Switch 1 of Mg^{2+}-free Arf1 was partially a loop, while that of the Mg^{2+}-bound form remains a β-sheet. It is notable that the mutation of Phe51 was reported to be critical for the GEF-binding.[15] As for Rab6, we were unable to compare its Mg^{2+}-free form with the GEF-bound form, because the X-ray crystallographic structure was unavailable. However, we speculate that Rab6−GEF will interact with a groove between the switch 1 and the GDP-binding site, similar to the H-Ras−SOS interaction. Judging from these findings on the structures of the Mg^{2+}-free GNBPs, it is concluded that the detachment of the Mg^{2+} ion has a keen role in inducing a conformational change of the GNBPs to prepare the template for the GEF binding.

It was reported that the point mutation of H-RasS17N, which was critical for the Mg^{2+} coordination, caused an increase of GEFs' affinity.[38] In addition, the chelation of the Mg^{2+} ion increased the affinity of H-Ras for SOS and enhanced the dissociation of GDP.[12,39] N-Ras, an isoform of H-Ras, had 10 times greater affinity for GTP than GDP at low Mg^{2+} concentrations, whereas the affinities of GTP and GDP were approximately the same at high Mg^{2+} concentrations.[19] Additionally, several mutational studies of other small G-proteins revealed the importance of the Mg^{2+} ion for the GEF binding. Rab3AT36N[40] and RanT24N[41] (analogous to H-RasS17N) mutants were indicated to have greater affinity for their respective GEFs than their wild-type had. All mutated residues in these mutants were demonstrated to be essential to the coordination of the Mg^{2+} ion. In the Rho family, it was proposed that GEF had a negative correlation with the free Mg^{2+} ion in the cell; thus, high concentrations of Mg^{2+} ion decreased GEF affinity for GNBPs.[42] The role of the Mg^{2+} ion for GDP binding was supposed to stabilize the GDP-binding state, since the presence of the Mg^{2+} ion prevented GDP dissociation in various GNBPs;[42,43] moreover, the picomolar levels of the Al^{3+} ion competed with the Mg^{2+} ion and inhibited the GDP/GTP exchange of Ras.[44] Furthermore, the crystallographic studies of GDI-bound GNBPs revealed that the GDIs inhibited GDP dissociation by stabilizing the Mg^{2+} binding.[44] The experimental data, all of the above, suggested that the detachment of the Mg^{2+} ion increases the affinity for GEFs and promotes the GDP dissociation.

Formerly, GEFs were assumed to promote GDP dissociation by disrupting the Mg^{2+} coordination.[46] But recently, some studies provided different viewpoints on the relationship between GEF and the Mg^{2+} ion. A structure-based mutagenesis study of H-Ras and SOS (Ras−GEF) proteins demonstrated that mutations of the residues in SOS, which were expected to disrupt the Mg^{2+}-binding site, had no effect on the catalytic function of SOS.[46] Furthermore, a fluorescence study on Rac, a member of Rho family, demonstrated that the release of Mg^{2+} ion led to the GDP dissociation in its GDP/GTP exchange reaction.[24] These studies indicated that the disruption of Mg^{2+} coordination was independent of GEFs and that the exchange reactions were dominated by the binding of GEFs to the Mg^{2+}-free but

(47) Alexov, E. G.; Gunner, M. R. *Biochemistry* **1999**, *38*, 8253.
(48) Nakano, T.; Kaminuma, T.; Sato, T.; Akiyama, Y.; Uebayasi, M.; Kitaura, K. *Chem. Phys. Lett.* **2000**, *318*, 614.

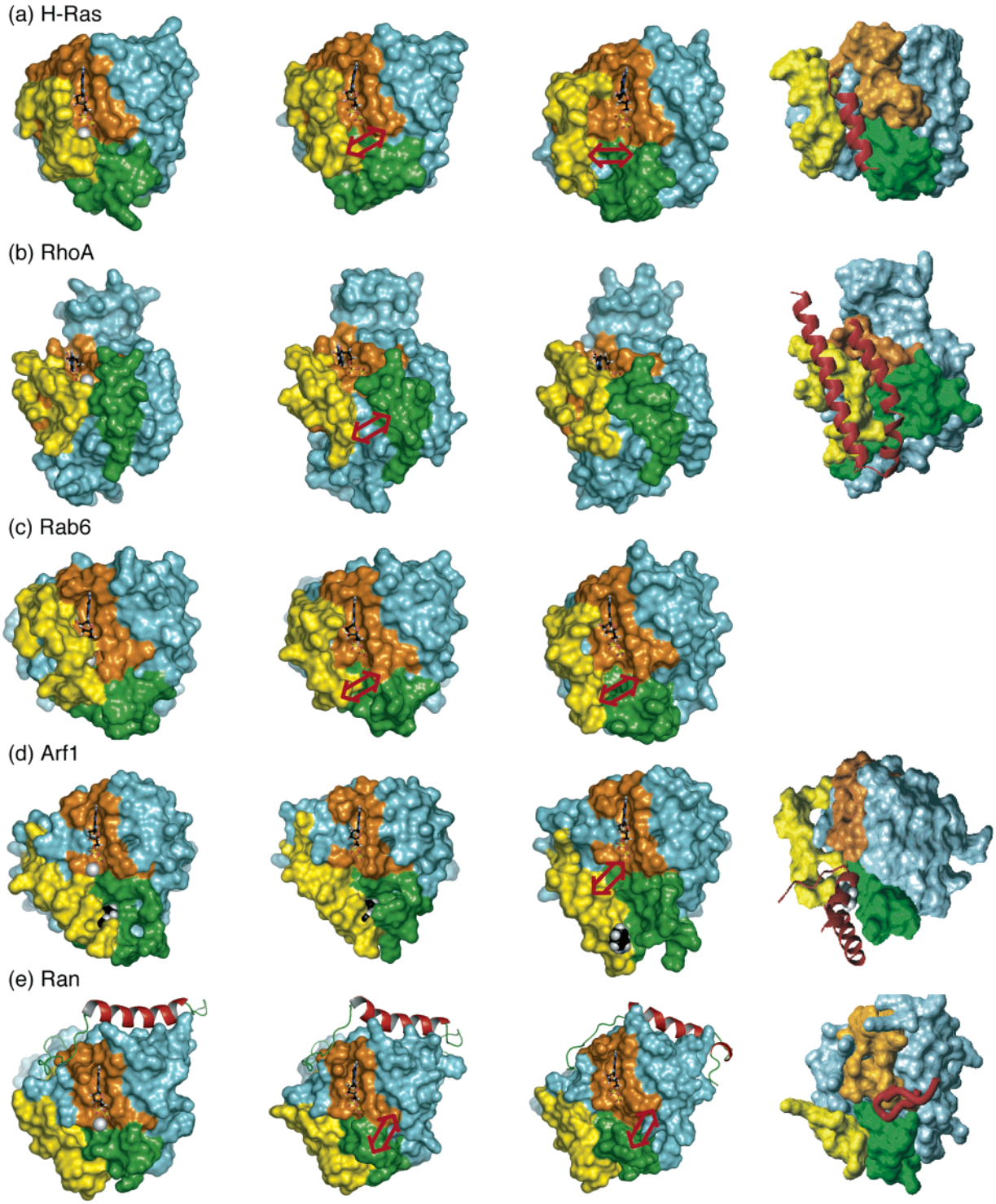

Figure 6. Solvent accessible surfaces of the average Mg^{2+}-bound, Mg^{2+}-free, Mg^{2+}-free (AMBER default protonation state), and GEF-bound GNBP structures (Left, Mg^{2+}-bound form; middle-left, Mg^{2+}-free form (pK_a-determined protonation state); middle-right, Mg^{2+}-free form in the AMBER default protonation state; right, GEF-bound form). GDPs are shown as a ball-and-stick representation. White spheres represent Mg^{2+} ions. The switch 1, the switch 2, and NBD regions are colored with yellow, green, and dark orange, respectively. The rest is sky blue. The helices or loops of GEFs are represented by red tubes. Red arrows indicate the grooves appearing due to the lack of Mg^{2+} ion. These time-average structures were obtained from the final 0.2 ns MD simulations.

nucleotide-bound GNBPs. That is, it can be speculated that the release of the Mg^{2+} ion induces the interaction of GEFs with GNBPs. Our present results provide a new semiopen model that can be a template for GEF binding. Moreover, our simulation revealed that the elimination of the Mg^{2+} ion converts the conformation of not only RhoA but also all members of the small G-proteins to the semiopen forms. Consequently, it is concluded that the Mg^{2+} ion regulates the conformation of the small G-proteins.

Mg^{2+} ions are universally present in a cell, and the concentration of the Mg^{2+} ion may locally change as Ca^{2+} ions do (due to various stimulations such as the elevation of cation, anion,

and ATP concentrations in the cell). The concentration of the Mg^{2+} ion possibly determines what states a small G-protein is, whether at the closed form when the Mg^{2+} concentration is high or at the semiopen form when the Mg^{2+} concentration is low.

Acknowledgment. We thank Dr. Goldberg for providing the coordinates of the Arf1−Gea2 complex and Ms. Nagara for preparing the manuscript. This research was financially supported by the Sasakawa Scientific Research Grant from The Japan Science Society. This work has been supported by a Grant-in-Aid for JSPS Fellows and a Grant-in-Aid for Center Of Excellence (COE) research from the Ministry of Education, Science, Sport, and Culture, Japan, and Japan Science and Technology Agency.

Supporting Information Available: Additional figures and tables (the RMSD plot, the detailed comparison of the calculated B-factors with the crystallographic temperature factors, the results using the AMBER default protonation state, the results of FMO calculation of H-Ras, the pK_a values calculated by MCCE, and the solvent accessible surface areas) are available in the Supporting Information. This material is available free of charge via the Internet at http://pubs.acs.org.

JA0467972